Available online at www.sciencedirect.com
SCIENCE DIRECT
Precambrian Research 147 (2006) 107–123
Precambrian Research
www.elsevier.com/locate/precamres

Multi-stage origin of the lower crust of the Karelian craton from 3.5 to 1.7 Ga based on isotopic ages of kimberlite-derived mafic granulite xenoliths

Petri Peltonen [a,*], Irmeli Mänttäri [a], Hannu Huhma [a], Martin J. Whitehouse [b]

[a] *Geological Survey of Finland, P.O. Box 96, FI-02151 Espoo, Finland*
[b] *Swedish Museum of Natural History, P.O. Box 50007, SE-10405 Stockholm, Sweden*

Received 9 November 2004; received in revised form 23 February 2006; accepted 24 February 2006

Abstract

Mafic garnet granulite xenoliths recovered from ~500 to 600 Ma old eastern Finland kimberlites provide direct information on the petrology and physical properties of the lower cust below the Archean Karelian craton. Mineral thermobarometry, together with isotopic, petrological and seismic velocity constraints, imply that the xenolith suite is derived from a geophysically-determined, dense, high-velocity layer at the base of the crust (40–58 km depth). Single grain zircon U–Pb dates and Nd model ages (T_{DM}) imply that this is a hybrid layer consisting of both Archean and Proterozoic mafic granulites. Zircon ages of up to ~3.5 Ga and Nd T_{DM} model ages ~3.7 Ga of the xenoliths are equivalent to those of the oldest upper crustal assemblages. During the Proterozoic, transient heating of these Archean granulites by voluminous basic magmatic intrusions resulted in multiple younger zircon generations within individual xenoliths. The most important post-Archean lower crust growth took place during ~1.9 Ga accretion of the Svecofennian arc complex to the craton margin, when underplating Proterozoic basaltic magmas became mingled with pre-existing Archean mafic granulites. Later, post-orogenic (~1.80–1.73 Ga) transient heating of the lower crust occurred as a response to magmas ponded at the uppermost lithospheric mantle. In conclusion, Karelian lower crust records the geological evolution of the craton margin environment through a period of nearly 4 billion years. Our data add a new piece to the emerging picture that emphasises the global importance of the 3.5 Ga crustal growth episode. We suggest that it represents a major mantle-plume event – more widespread than previously recognized – when a significant fraction of Paleoarchean continental crust was formed.

Keywords: Lower crust; Mafic xenoliths; Zircon; Nd–Sr–Pb isotopes; Kimberlite; Paleoarchean; Proterozoic; Recrystallisation; Mantle-plume; Craton; Finland

1. Introduction

The lower crust of Archean cratons remains a poorly characterised realm. Although exposed Archean granulites are relatively common, it is not always evident whether they represent lowermost continental crust or granulites formed at transient high pressure–temperature conditions during continent–continent collisions (Rudnick, 1992). Therefore, xenolith suites which show clear evidence for their derivation from the present lower crust of Archean cratons provide invaluable insight into the nature of the first continents on Earth. Such xenoliths may bear fundamental information on the growth mechanism of Archean crust, allow more accurate estimates of its total volume

* Corresponding author.
E-mail addresses: petri.peltonen@gtk.fi (P. Peltonen), irmeli.manttari@gtk.fi (I. Mänttäri), hannu.huhma@gtk.fi (H. Huhma), martin.whitehouse@nrm.se (M.J. Whitehouse).

0301-9268/$ – see front matter © 2006 Elsevier B.V. All rights reserved.
doi:10.1016/j.precamres.2006.02.008

to be made, and may help to constrain the origin of the underlying lithospheric mantle root, and indicate whether it has remained coupled with the crust through the geological history of the Archean craton.

Lower crustal xenoliths were recovered from the 500 to 600 Ma old Kaavi-Kuopio kimberlites, that intruded the Archean crust and Proterozoic cover sediments of the Karelian craton some 80 km inwards from the craton to mobile belt suture (Fig. 1a). This xenolith suite is particularly valuable since it provides us direct access to the chemical composition, physical state and age of the lower crust of the Karelian craton. Hölttä et al. (2000) obtained pressure–temperature estimates and mineral analytical data for a subset of this sample suite. They also reported preliminary U–Pb zircon dates and Sm–Nd analyses for two xenoliths. For the sake of completeness, these data are included in tables and diagrams of this study. Other relevant studies include those from xenolith samples representing the lower crust of the late Archean Belomorian mobile belt between the Karelian and Kola

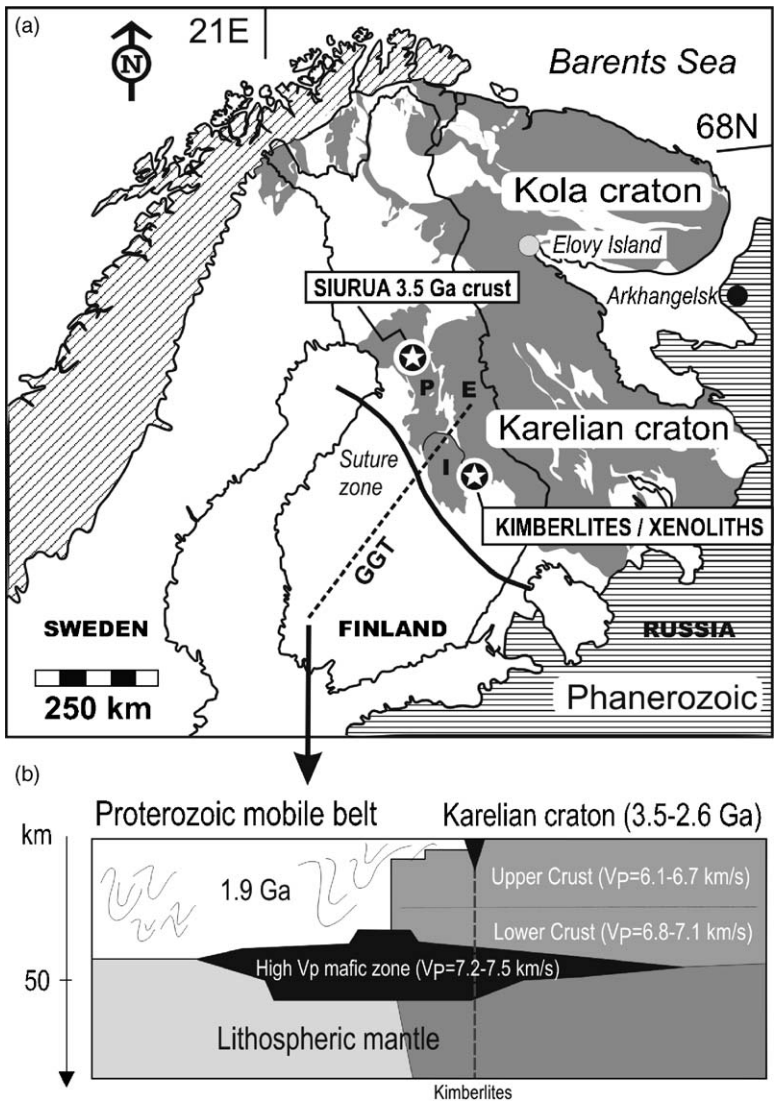

Fig. 1. (a) Generalised geological map of the Fennoscandian Shield showing the location of the granulite xenolith-bearing kimberlites, and the oldest known upper crust locality at Siurua. Shaded area are the Archean granite-greenstone terrains of the Kola and Karelian cratons and white are post-Archean, mainly Svecofennian rocks. Other abbreviations: global geoscience transect-line (GGT); Iisalmi block (I), Pudasjärvi block (P), and Eastern Finland complex (E). (b) Cross-section along the GGT-profile (fourfold vertical exaggeration) as modified from Korsman et al. (1999). Only the upper part of the lithospheric mantle is shown, its total thickness exceeding 240 km at this locality (Kukkonen and Peltonen, 1999). Note that the P-wave velocities of the high-velocity mafic unit match with those calculated for the mafic garnet granulite xenoliths (Table 1).

cratons, recovered from the Elovy island (Fig. 1a) diatremes (Markwick and Downes, 2000; Kempton et al., 2001; Downes et al., 2002).

Here, we provide ion probe U–Pb zircon dates for six mafic granulite xenoliths from eastern Finland kimberlites, and Nd, Sr, and Pb isotope analyses of 13 samples. We demonstrate that the lower crust of the Karelian craton is hybrid in composition: it contains 3.5 Ga old granulites (remnants of the lower crust of the protocontinent?), which were intruded by basaltic magmas causing a series of transient heating events during the Neoarchean and Paleoproterozoic.

2. Geological setting

The Karelian craton forms a coherent, mainly Meso- to Neoarchean cratonic nucleus, 200,000 km^2 in size, in eastern and northern Finland and adjacent northwest Russia (Fig. 1a). Majority of the greenstone belts and TTG series intrusive rocks and migmatites were formed between 2.7 and 2.9 Ga, while a minor older component dates back to 3.1–3.2 Ga (for a review see Sorjonen-Ward and Luukkonen, 2005 and references therein). Recently, the fragmentary evidence for the presence of Paleoarchean crust (based on Nd model ages and detrital zircons; e.g. Claesson et al., 1993) has been supported by a ~3.5 Ga protolith magmatic age obtained for trondhjemitic orthogneiss in central Finland (Fig. 1a; Mutanen and Huhma, 2003). Case studies have proposed distinct origins for individual greenstone belts: oceanic plateau for the Kostomuksha (Puchtel et al., 1998), island arc for the Sumozero-Kenozero (Puchtel et al., 1999) and continental rift zone origin for the Kuhmo-Suomussalmi belt (Luukkonen, 1992). The North Karelian greenstone belt (Iringora structure) preserves distinctive features of an ophiolite pseudostratigraphy (Shchipansky et al., 2004). Such diversity suggests a complex – so far poorly constrained – accretionary history during the Archean.

Layered intrusions, dyke swarms and volcanic rocks record discrete events of cratonic extension at 2.45, 2.3, 2.2, 2.1 and 1.97 Ga (Vuollo and Huhma, 2005). Some uncertainty exists whether it was the ~2.1 or ~1.97 Ga event that led to break-up of the proto-craton, and formation of the passive nonvolcanic continental margin at the present southwest edge of the craton (Peltonen and Kontinen, 2004). The present structure of the craton margin has been formed by progressive collision of two juvenile arc complexes with the cratonic nucleus between 1.91 and 1.87 Ga, an event that resulted in tectono-thermal overprinting and fragmentation of the cratonic marginal basement into several megasize blocks (Nironen, 1997; Sorjonen-Ward and Luukkonen, 2005). The craton margin is characterised by unusually thick crust (up to 58 km) which progressively thins both towards the core of the craton (~42 km) and towards the Svecofennian mobile belt. Seismic surveys imply that upper crust has a relatively uniform thickness in Fennoscandia, and that the Moho depth variations are mainly due to thickness variations within the 0–30 km thick high-velocity layer (V_P > 7.0–7.5 km/s) at the base of the crust (Fig. 1b). Combined with Bouguer anomaly data, the seismic constraints require that the lower crust has a density contrast of +300–350 kg/m^3 relative to the upper crust, and −200–300 kg/m^3 contrast relative to the upper mantle (Korsman et al., 1999). These values emphasize the mafic bulk composition of the lower crust.

Recently, Kuusisto et al. (2006) studied the lithology of the deep crust at this locality using seismic wide-angle velocity models and laboratory measurements on P- and S-wave velocities of different rock types. Their study implies that the crust becomes gradually more mafic with increasing depth and that velocity profiles require more mafic composition than an average global continental model would suggest. Modeling of Kuusisto et al. (2006) suggests that a lower crust consisting only of a single rock type is incompatible with the seismic data, but rather the best fit was obtained with a lower crust consisting of a mixture of mafic garnet granulites, hornblendites, pyroxenites, tonalitic gneiss and minor eclogites. With the exception of eclogites all these rock types are present also in our lower crustal xenolith suite.

3. Samples

Twenty-two lower crustal granulite xenoliths were recovered from 500 to 600 Ma old Eastern Finland kimberlites, which intrude at the Karelian craton margin ~80 km inwards from the craton to mobile belt suture zone (O'Brien and Tyni, 1999). Twenty-one of these samples were picked from non-processed bulk mine samples of Pipe #7 (Lahtojoki), and the remaining sample (Ju11) was extracted by diamond saw from 45 mm diameter drill core material of Pipe #14 (Kaatronlampi), ca. 10 km northwest from Pipe #7. While a lower crustal origin is evident for mafic garnet-bearing granulite xenoliths, this is less evident for other, garnet-free lithologies. To avoid biased sampling we also examined several hundreds of rounded xenoliths other than mafic garnet granulites. The degree of roundness is likely to roughly correlate with the time of the mechanical abrasion by the kimberlite and thus with the depth of origin for a xenolith. We prepared several tens of polished thin sections of the most rounded garnet-free xenoliths, six of which (gab-

Table 1
Sample information of the studied lower crustal xenoliths from the Kaavi-Kuopio kimberlites (Eastern Finland)

Sample	Rock type	Description	Modes	V_P[b] (km/s)	U–Pb dating (Table 2)	Nd–Sr–Pb isotope data (Table 3)
L81	Mafic garnet granulite	Granoblastic-polygonal	Grt_{17} Cpx_{48} Am_1 Pl_{27} Op_3 Qtz_3 (Scp)	7.326		
7HH	Mafic garnet granulite	Granoblastic-polygonal	Grt_{15} Cpx_{38} Am_4 Pl_{42} (Op, Qtz, Zr)[a]	7.244	+	+
L87	Mafic garnet granulite	Weakly banded, granoblastic-polygonal	Grt_{18} Cpx_{32} Am_9 Pl_{33} Op_7 (Ap, Zr)	7.343	+	+
X001	Mafic garnet granulite	Weakly banded, granoblastic-polygonal	Grt_{21} Cpx_{32} Am_{10} Pl_{31} Op_6 (Ap, Qtz)	7.320		+
L23	Mafic garnet granulite	Granoblastic, some alteration	Grt_{14} Cpx_{30} Am_{10} Pl_{39} Op_6 Qtz_1 (Zr)	7.172		
L94	Mafic garnet granulite	Granoblastic-polygonal, weak alteration	Grt_{27} Cpx_{29} Am_{11} Pl_{26} Op_5 Qtz_2 (Zr)[a]	7.484	+	+
L88	Mafic garnet granulite	Porphyroblastic garnet, partly recrystallised	Grt_{13} Cpx_7 Am_{19} Pl_{54} Chl_4 Op_2 (Ap, Zr)[a]	6.950	+	+
L83	Mafic garnet granulite	Cumulate texture	Grt_{22} Cpx_{23} Am_{31} Pl_{20} Op_4 (Zr)	7.386		
L91	Mafic garnet granulite	Granoblastic-polygonal	Grt_{19} Cpx_{27} Am_{32} Pl_{19} Op_3 (Ap)[a]	7.412		+
R-38-193	Mafic garnet granulite	Banded, some alteration	Grt_{15} Cpx_{27} Am_{34} Pl_{21} Op_3 (Ap)	7.300		
X002	Mafic garnet granulite	Coarse grained	Grt_{26} Cpx_{21} Am_{37} Pl_9 Op_7 (Ap)	7.527		+
L84	Mafic garnet granulite	Some alteration	Grt_{20} Cpx_{11} Am_{47} Pl_{19} Op_3	7.311		
L85	Mafic garnet granulite	Cumulate texture	Grt_{19} Cpx_{25} Am_{47} Pl_5 Op_4 (Ap, Zr)	7.473		
L73	Mafic garnet granulite	Replacive amphibole	Grt_9 Cpx_{16} Am_{52} Pl_{19} Chl_3 (Op, Zr)[a]	7.284	+	+
X006	Mafic garnet granulite	Granoblastic-polygonal	Grt_{20} Cpx_4 Am_{59} Pl_{17}	7.289		
Ju11/15.95	Mafic garnet granulite	Granoblastic-polygonal	Grt_{20} Cpx_{15} Pl_{65} (Zr, Mnz)	6.997	+	+
L104	Mafic granulite (gabbro)	Recrystallised igneous texture, strained	Cpx_{16} Opx_{19} Pl_{48} Bt_{14} Qtz_2 (Ap, Zr)	6.574		+
X208	Felsic granulite (monzodiorite)	Recrystallised igneous texture, porphr. opx	Opx_4 Am_2 Pl_{63} Bt_6 Qtz_4 Kfs_{19} Op_2	6.371		+
L96	Felsic granulite (tonalite)	Recrystallised igneous texture	Opx_4 Am_{12} Pl_{50} Bt_1 Qtz_{32} (Ap, Op, Cpx, Zr)	6.392		
L89	Pyroxene-hornblende gabbro	Cumulate texture	Cpx_7 Am_{77} Pl_{14} Op_1 (Zr)	7.075		+
X029	Pyroxene-hornblende gabbro	Myrmekitic and granophyric intergrowths	Cpx_{25} Am_9 Pl_{39} Bt_9 Op_7 Qtz_{11}	6.630		+
L82	Hornblende gabbro	Cumulate texture	Am_{75} Pl_{22} Op_3 (Ap, Zr)	6.993		

Modes are based on point-counting of ca. 1500 points/polished thin section; Grt: garnet; Cpx: clinopyroxene; Opx: orthopyroxene; Am: amphibole (hornblende); Pl: plagioclase; Op: opaques; Qtz: quartz; Ap: apatite; Bt: biotite; Ttn: Titanite; Mnz: monazite; Zr: zircon; Kfs: potassium feldspar; Scp: scapolite; Chl: chlorite.

[a] Modes After Hölttä et al. (2000).

[b] P-wave velocities calculated from modal compositions for pressure of 0.97 GPa and temperature of 347 °C taken from Kuusisto et al. (2006).

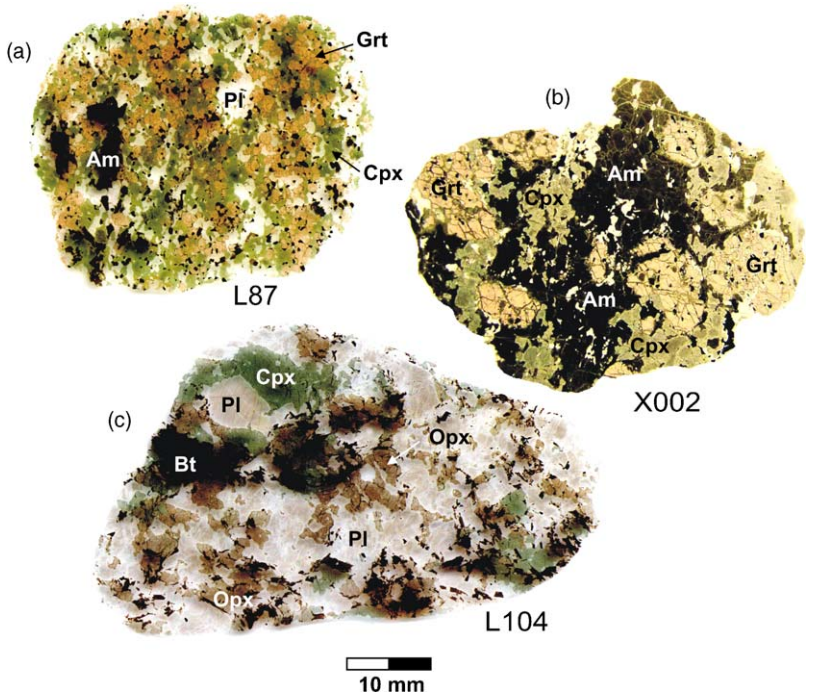

Fig. 2. Microphotographs of the (a) garnet granulite xenolith L87 that yielded >3.5 Ga zircon grains, (b) amphibole-rich garnet granulite X002, and (c) garnet-free orthopyroxene-rich granulite xenolith ("gabbro") that yielded the oldest Nd T_{DM} age of ~3.7 Ga.

bros and tonalitic granulites) turned out to contain either mineralogical or textural evidence for lower crustal origin, and were included in this study (Table 1). Other lithologies, for example metapelites, seem to be absent from the lowermost crust.

Mafic garnet granulites, which are well-rounded xenoliths 1–8 cm in diameter, consist of garnet, clinopyroxene, amphibole and plagioclase (Table 1). Magnetite and ilmenite are frequently present; quartz, apatite and zircon are common accessories. The mineralogy is fresh and xenoliths have granoblastic texture with 120° triple junctions (Fig. 2a), a prominent schistosity is absent but several samples show mineralogical banding. Some samples contain porphyroblastic garnet that encloses all other mineral. The characteristic feature of mafic garnet granulites is the abundance (mean: 27%) of dark green to dark brown amphibole (tschermakitic to pargasitic hornblende). Amphibole is strongly pleochroic and sometimes only weakly transparent due to abundant ilmenite exolutions. Textural observations and mineral compositions rule out its secondary retrograde origin. In some xenoliths amphibole grains are similar to cumulus grains while in other samples amphibole and plagioclase show curved mutual grain boundaries that resembles the peritectic reaction between cumulus plagioclase crystals and post-cumulus amphibole observed in layered intrusions. Petrographically, mafic granulites give the impression of a magmatic suite of rocks, where igneous textures with increasing degree of recrystallisation grade into texturally highly equilibrated granoblastic rocks. Hölttä et al. (2000) report the following temperature and pressure estimates for the Grt–Cpx–Pl–Qtz assemblage using TWEEQU-software and mineral core compositions: $T = 800–930\,^{\circ}C$ (mean of 840 °C, $n = 12$) and $P = 0.84–1.25$ GPa (mean of 1.0 GPa, $n = 12$). The significance of these estimates is discussed in more detail in Section 6.1. "*Depth of origin and thermal history of the lower crustal xenoliths*".

Garnet-free lower crustal xenoliths (L96, X208, and L104) are orthopyroxene-bearing mafic (gabbro) or felsic (monzodiorite or tonalite) granulites with strained and recrystallised plutonic texture (Fig. 2b).

Modal compositions of *gabbroic xenoliths* (L89, X029, and L82) are similar to those of mafic granulites, except that they do not contain garnet. They contain abundant amphibole similar to that in garnet granulites, but exhibit a more distinct cumulus-texture than mafic granulites. We interpret them to belong to the same igneous suite of basic rocks as the garnet granulites. Gabbro xenolith X029 is distinct from the other two: it exhibits a subophitic texture and complex graphic intergrowths between plagioclase and clinopyroxene, and between plagioclase and quartz. The origin of such textures in unknown but may be indicative of the xenolith

origin from the marginal (granophyre) unit of a slowly cooled mafic intrusive bodies.

4. Analytical methods

Samples had their outer surfaces removed and then were cut into thin slices by a diamond saw. Slices were crushed by hammer and pulverised in a carbon steel bowl, known to be free of elements other than Fe and Mn. Some samples were crushed and garnet, clinopyroxene and plagioclase were separated using standard mineralogical techniques. The small size of the xenoliths limited the number of samples suitable for mineral separation.

For Sm–Nd and Rb–Sr analyses the handpicked mineral concentrates (ca. 100–200 mg) were washed ultrasonically in warm 6 N HCl for 30 min, and rinsed several times in water. The samples were dissolved in HF–HNO_3 using Savillex screw cap teflon beakers or teflon bombs for 48 h. Mixed ^{149}Sm–^{150}Nd and ^{87}Rb–^{84}Sr spikes were added to the sample prior the dissolution. The concentrations were measured by isotope dilution, and chemical separations were carried out using standard chemical procedures. The measurements have been made in a dynamic mode on a VG SECTOR 54 mass-spectrometer using triple filaments (Sm and Nd), single Re filament (for Pb and most garnet Nd) or single Ta filament (Sr). The estimated error in $^{147}Sm/^{144}Nd$ is 0.4%, and for $^{87}Rb/^{86}Sr$ 0.6%. $^{143}Nd/^{144}Nd$ ratio is normalized to $^{146}Nd/^{144}Nd = 0.7219$, and $^{87}Sr/^{86}Sr$ to $^{86}Sr/^{88}Sr = 0.1194$. The average value for the La Jolla standard is $^{143}Nd/^{144}Nd = 0.511850 \pm 7$ (std, $n = 70$, triple filament measurements), and for SRM987 $^{87}Sr/^{86}Sr = 0.710250 \pm 25$ (S.D., $n = 20$). Compared to triple filament measurements the single Re-filament analyses on several samples and standard provided slightly lower (0.005%) $^{143}Nd/^{144}Nd$ ratios. The single filament measurements have been corrected accordingly, and should be compatible with the La Jolla value of 0.51185. The average error in ε_{Nd} is 0.5 units. T_{DM} is calculated according to DePaolo (1981). The ε_{Sr} has been calculated using reference values of $^{87}Rb/^{86}Sr = 0.0816$ and $^{87}Sr/^{86}Sr = 0.7045$. Measurement on the rock standard BCR-1 provided the following values: Sm = 6.58, Nd = 28.8 ppm $^{147}Sm/^{144}Nd = 0.1380$, $^{143}Nd/^{144}Nd = 0.51264 \pm 0.00002$, Rb = 47.1 ppm, Sr = 330 ppm, $^{87}Rb/^{86}Sr = 0.412$, $^{87}Sr/^{86}Sr = 0.70502 \pm 0.0002$. The average blank measured during mineral analyses was: 50 pg for Sm, 150 pg for Nd, 100 pg for Rb, and 300 pg for Sr.

Subsamples for U–Pb dating of single zircon grains were first cut into thin slices with diamond saw. Slices were carefully crushed in a pre-cleaned shatter-box and wet-sieved using disposable sieve cloth. The heavy mineral fraction was extracted from the 70 to 200 mesh fraction using heavy liquids, and zircons were handpicked from the concentrate. The selected zircons were mounted in epoxy, polished and coated with carbon for SEM study, and with gold for SIMS analysis. The ion microprobe U–Pb analyses were made using the Nordic Cameca IMS 1270 at the Swedish Museum of Natural History, Stockholm, Sweden. The spot-diameter for the 4 nA primary O_2^- ion beam was ca. 25 μm and oxygen flooding in the sample chamber was used to increase the production of Pb^+ ions. Four counting blocks, each including three cycles of Zr, Pb, Th, and U masses of interest were measured from each spot. The mass resolution ($M/\Delta M$) was 5400 (10%). The raw data were calibrated against a zircon standard 91500 (Wiedenbeck et al., 1995) and corrected for modern common lead ($T = 0$; Stacey and Kramers, 1975). For the detailed analytical procedure see Whitehouse et al. (1999). Plotting of the U–Pb isotopic data and calculating the concordia and intercept ages were done using the Isoplot/Ex program (rev. 2.49; Ludwig, 2001). The data-point error ellipses in the concordia diagrams are 2σ. All the errors in age results are 2σ errors with decay constant errors ignored.

5. Results

5.1. U–Pb ages

Most zircons, with the exception of some grains from the dry (i.e. amphibole-free) mafic granulite (Ju11), lack overgrowths larger than the beam size, and thus all dates represent core analyses unless otherwise stated.

Sample L87 (mafic granulite) yielded 87 grains of zircon that can be subdivided into two types. Most zircons (85) are 60–150 μm in size, clear and colorless, rounded grains with no visible zoning in transparent light or BSE images (Fig. 3a). Such grains are extremely low in U (6–16 ppm), Th and Pb, and yield imprecise ages of ca. 1.8 Ga. Two zircons grains are distinct in showing pink color, clear igneous zoning in transparent light (but only weak in BSE images), and have high U (320–422 ppm), Th and Pb abundances. They yield early Archean $^{207}Pb/^{206}Pb$ ages of 3467 ± 10 and 3477 ± 10 Ma (Fig. 3; Table 2).

Fifty grains were extracted from mafic granulite sample L88. These show greater textural and compositional diversity than L87 grains. In addition to oval grains similar to those in sample L87, prismatic crystals with variably rounded tips occur (Fig. 3b). Zoning can be clearly

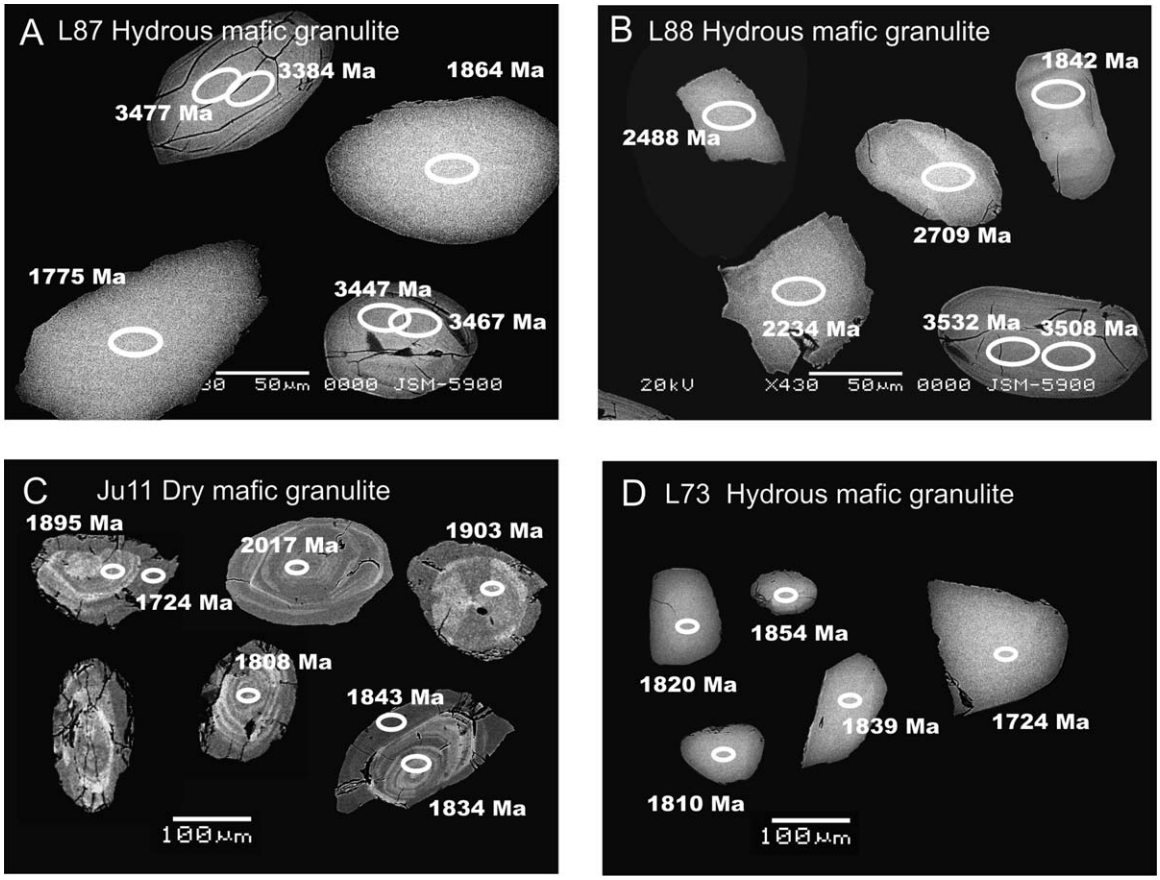

Fig. 3. Backscattered electron images of representative zircons from mafic garnet granulite xenoliths showing analysis spots with age (Ma).

visible, diffuse or absent, gradually decreasing from brown to colorless grains. The more anhedral and clear zircons have more diffuse zoning and lower uranium contents. In accordance with such textural diversity, L88 grains yielded a large range of ages. The $^{207}Pb/^{206}Pb$ age of 3532 ± 10 Ma obtained from brown, prismatic zoned grain 01 (363 ppm U) is the oldest age recorded by this xenolith suite. Five grains form a tight population at ~1870 Ma, while the remaining seven zircons record a plethora of $^{207}Pb/^{206}Pb$ ages between these Archean and Proterozoic "endmembers" (Fig. 4).

Amphibole-free dry mafic granulite Ju11/15.95 yielded abundant zircon (Fig. 3c). The grains are clear and light pink in color, some are brownish. Grains are fractured and their outer surfaces are corroded. Magmatically zoned grain cores can be surrounded by a lighter, featureless, metamorphic zircon rim. Some grains are unzoned and low in uranium and may represent thoroughly recrystallised old grains or newly formed zircon (Mezger and Krogstad, 1997). One grain core records a $^{207}Pb/^{206}Pb$ age of 2500 Ma, the remaining cores range from 1808 to 2017 Ma. Grain 05 records a distinctly younger rim (1724 ± 32 Ma) versus older core age of 1895 ± 14 Ma.

Mafic granulite L73 yielded only clear and colorless, elongated to oval grains that almost completely lack internal features. Some grains show heavier (brighter at BSE) inner domains surrounded by lighter (darker) zircon, but no clear igneous zoning is present (Fig. 3d). Within error all U–Pb ages are concordant at 1.8–1.85 Ga.

5.2. *Nd–Sr–Pb isotope data*

Whole rocks (wr) and mineral separates (Pl, Cpx, Grt) representing 13 lower crustal xenoliths were analysed for Sm–Nd, Rb–Sr, and Pb isotopes (Table 3). In order to avoid contamination with the kimberlite host only interior parts of the xenoliths were used for whole rock analysis. As garnet and clinopyroxene analyzed were clear and fresh, we are confident that they are free of contamination. Clinopyroxene is a major REE carrier with Sm/Nd close to whole rock, and the Sm–Nd data on both Cpx and wr may thus be used for evaluating the crustal residence

Table 2
Ion microprobe zircon U–Pb isotopic data from mafic lower crustal xenoliths, Finland

Sample/spot #	Derived ages						Calibrated ratios						Rho	Disc. (%)	Elemental data			$^{206}Pb/^{204}Pb$
	$^{207}Pb/^{206}Pb$	$\pm s$	$^{207}Pb/^{235}U$	$\pm s$	$^{206}Pb/^{238}U$	$\pm s$	$^{207}Pb/^{206}Pb$	$\pm s$ (%)	$^{207}Pb/^{235}U$	$\pm s$ (%)	$^{206}Pb/^{238}U$	$\pm s$ (%)			[U] (ppm)	[Th] (ppm)	[Pb] (ppm)	
L87																		
n899-01a	1546	76	1660	38	1752	30	0.0959	4.16	4.129	4.60	0.3122	1.96	0.43		6	3	2	1.65E+03
n899-02a	1775	48	1795	28	1813	29	0.1085	2.69	4.860	3.26	0.3248	1.83	0.56		8	4	3	8.13E+03
n899-03a	1864	31	1861	21	1859	28	0.1140	1.71	5.254	2.43	0.3344	1.73	0.71		16	9	7	9.48E+03
n899-04a	3447	4	3301	16	3065	40	0.2956	0.25	24.803	1.67	0.6087	1.65	0.99	−10.9	422	134	353	1.35E+04
n899-04b	3467	5	3348	16	3152	41	0.2994	0.30	26.037	1.67	0.6307	1.64	0.98	−8.4	392	122	341	1.25E+04
n899-05a	3384	5	3327	17	3233	43	0.2838	0.31	25.479	1.70	0.6512	1.67	0.98	−2.3	320	118	287	6.27E+03
n899-05b	3477	4	3423	17	3333	44	0.3013	0.25	28.123	1.69	0.6770	1.68	0.99	−2.0	412	156	392	9.39E+03
L88																		
n897-01a	3508	4	3509	17	3511	45	0.3074	0.24	30.687	1.67	0.7239	1.66	0.99		363	119	366	3.63E+04
n897-01b	3532	5	3527	17	3520	45	0.3122	0.32	31.265	1.69	0.7264	1.66	0.98		296	97	301	9.81E+04
n897-02a	1876	10	1861	15	1848	27	0.1148	0.55	5.254	1.74	0.3321	1.65	0.95		229	70	91	1.18E+04
n897-03a	2606	12	2637	17	2678	37	0.1750	0.73	12.428	1.83	0.5151	1.67	0.92		39	86	37	2.06E+04
n897-04a	2234	16	2161	18	2084	30	0.1406	0.94	7.399	1.94	0.3817	1.70	0.87	−2.8	35	84	25	1.60E+04
n897-05a	1875	14	1842	16	1813	26	0.1147	0.79	5.137	1.84	0.3248	1.66	0.90		125	50	50	1.59E+03
n897-07a	2488	22	2465	20	2437	35	0.1631	1.31	10.331	2.16	0.4595	1.71	0.80		30	61	24	9.09E+02
n897-08a	1842	27	1816	19	1794	26	0.1126	1.51	4.982	2.26	0.3208	1.68	0.74		193	58	73	3.42E+02
n897-09a	1863	6	1880	15	1895	27	0.1139	0.34	5.368	1.68	0.3417	1.65	0.98		508	48	198	5.06E+03
n897-10a	2709	12	2694	17	2673	36	0.1863	0.73	13.197	1.81	0.5139	1.65	0.91		118	103	86	6.15E+02
n897-11a	2889	12	2482	19	2016	34	0.2079	0.74	10.528	2.07	0.3672	1.94	0.93	−31.3	638	130	363	1.43E+02
n897-12a	1883	9	1904	15	1924	27	0.1152	0.51	5.525	1.72	0.3478	1.64	0.95		155	45	65	1.83E+04
n897-13a	2085	8	2021	15	1959	28	0.1291	0.48	6.319	1.71	0.3550	1.64	0.96	−3.4	399	177	183	8.99E+02
n897-14a	2196	6	1922	15	1679	24	0.1375	0.34	5.640	1.68	0.2975	1.64	0.98	−23.9	377	124	146	5.80E+02
JU11																		
n1040-01a	2017	11	1990	27	1963	51	0.1242	0.60	6.095	3.07	0.3559	3.01	0.98		155	149	77	4.32E+04
n1040-02a	1903	11	1878	26	1855	48	0.1165	0.61	5.356	3.05	0.3335	2.99	0.98		265	57	104	1.67E+05
n1040-03a	1834	8	1805	26	1781	47	0.1121	0.46	4.918	3.01	0.3181	2.98	0.99		519	241	205	2.95E+04
n1040-03b	1843	15	1853	27	1862	48	0.1127	0.82	5.203	3.09	0.3349	2.98	0.96		216	50	85	>1e6
n1040-04a	1808	10	1774	26	1746	47	0.1105	0.55	4.741	3.10	0.3111	3.05	0.98		262	101	99	8.55E+04
n1040-05a	1895	7	1864	26	1836	48	0.1160	0.41	5.267	3.03	0.3294	3.00	0.99		334	140	136	1.89E+04
n1040-05b	1724	16	1719	26	1714	45	0.1056	0.87	4.433	3.10	0.3045	2.97	0.96		106	39	39	6.35E+03
n1040-06a	2500	9	2393	29	2270	58	0.1642	0.55	9.557	3.08	0.4221	3.03	0.98	−5.1	215	179	126	5.38E+04
n1040-07a	1861	11	1804	26	1754	46	0.1138	0.62	4.908	3.06	0.3127	3.00	0.98	−0.3	193	31	70	4.41E+04
L73																		
n898-01a	1796	15	1781	16	1769	26	0.1098	0.84	4.780	1.86	0.3158	1.66	0.89		109	53	43	2.30E+03
n898-02a	1820	20	1807	17	1795	26	0.1113	1.10	4.928	1.99	0.3212	1.66	0.83		60	18	23	2.08E+03
n898-03a	1854	9	1858	15	1862	27	0.1134	0.50	5.234	1.72	0.3348	1.65	0.96		206	98	86	1.32E+04
n898-04a	1839	30	1810	20	1785	26	0.1124	1.68	4.944	2.39	0.3190	1.69	0.71		18	5	7	1.70E+04
n898-05a	1724	40	1785	24	1838	29	0.1055	2.22	4.802	2.86	0.3300	1.81	0.63		24	6	9	2.09E+04
n898-06a	1794	21	1810	17	1824	26	0.1097	1.15	4.948	2.02	0.3271	1.66	0.82		39	26	16	>1e6
n898-07a	1810	17	1855	16	1895	27	0.1106	0.94	5.212	1.91	0.3417	1.66	0.87		54	16	22	3.72E+04

L94																			
n154-01a	1766	36	1773	48	1778	82	0.1080	1.98	4.730	5.58	0.3177	5.21	0.93		25	6	9	>1e6	
n154-02a	1872	35	1798	48	1734	80	0.1145	1.94	4.873	5.56	0.3087	5.21	0.94		22	6	8	>1e6	
n154-03a	1783	31	1818	48	1848	85	0.1090	1.73	4.990	5.52	0.3321	5.25	0.95		29	9	11	>1e6	
n154-05a	1894	32	1850	48	1811	84	0.1159	1.79	5.183	5.56	0.3243	5.26	0.95		26	8	10	3.23E+04	
n154-06a	1980	93	1775	65	1605	74	0.1216	5.42	4.741	7.50	0.2828	5.19	0.69		3	1	1	8.31E+02	
n154-07a	1833	14	1902	46	1965	89	0.1121	0.76	5.507	5.25	0.3564	5.20	0.99		179	139	85	1.43E+04	
7HH																			
n155-01a	1779	70	1764	57	1750	81	0.1088	3.94	4.679	6.57	0.3119	5.26	0.80		10	3	4	2.96E+03	
n155-02a	1192	106	1507	62	1742	81	0.0798	5.56	3.413	7.68	0.3102	5.30	0.69	11.6	7	2	2	6.50E+03	
n155-03a	1834	56	1758	53	1696	80	0.1121	3.13	4.650	6.17	0.3009	5.32	0.86		9	2	3	1.06E+04	
n155-04a	2393	20	2253	49	2102	94	0.1542	1.16	8.196	5.33	0.3855	5.20	0.98	−4.1	72	41	36	2.76E+04	
n155-05a	1883	25	1901	47	1918	87	0.1152	1.42	5.504	5.40	0.3465	5.21	0.96		36	11	15	>1e6	
n155-06a	2332	20	2323	50	2314	103	0.1488	1.20	8.858	5.38	0.4318	5.25	0.98		88	28	47	>1e6	
n155-07a	2293	11	2239	48	2180	97	0.1454	0.65	8.067	5.24	0.4024	5.20	0.99		153	60	77	>1e6	
n155-08a	2668	6	2676	50	2685	115	0.1817	0.36	12.943	5.21	0.5167	5.19	1.00		701	230	459	9.12E+04	
n155-09a	1937	36	1927	50	1918	87	0.1187	2.05	5.672	5.61	0.3465	5.22	0.93		29	9	12	>1e6	
n155-10a	2637	4	2631	50	2622	113	0.1783	0.24	12.343	5.20	0.5020	5.19	1.00		1105	425	710	4.70E+04	
n155-11a	2310	10	2240	48	2165	96	0.1469	0.60	8.083	5.23	0.3991	5.19	0.99		190	94	97	7.76E+04	

All errors are at 1σ level. Degree of discordance is calculated at the closest 2σ limit.

time (Table 3; Fig. 5). Clinopyroxenes in samples L87 and L88 which contained Archean (>3.4 Ga) zircons, yield negative $\varepsilon_{Nd}(1900)$ values and Archean model ages (T_{DM}) of 3.0 Ga and 3.37 Ga, respectively, excluding the possibility that the old zircons are xenocrysts in the Proterozoic granulite. Similar results were obtained from sample 7-HH by Hölttä et al. (2000), in which, however, the analysis on wr very likely indicates significant kimberlite contamination in contrast to Cpx (Fig. 5). Samples which lack Archean zircon grains (Ju11, L73, L94), in turn, yield $\varepsilon_{Nd}(1900) \geq 0$ and Proterozoic T_{DM} ages. Most xenoliths have broadly similar subchondritic Sm/Nd ratios, but provide a large range of model ages. These results together with the zircon ages suggest that the lower crust consists of mingled Archean and Proterozoic granulites.

The Sm–Nd analyses on garnet–clinopyroxene pairs from three mafic granulite samples give ages of 1719 ± 9 Ma (L-91), 1692 ± 10 Ma (L-87) and 1604 ± 8 Ma (7-HH, Hölttä et al., 2000). These ages are significantly younger than any of the protolith ages (Table 3).

Sample L-87 yielded a clinopyroxene–plagioclase Rb–Sr isochron age of 454 ± 19 Ma with an initial ratio of $^{87}Sr/^{86}Sr = 0.702806 \pm 0.000046$ ($\varepsilon_{Sr} = -16.6$, Fig. 6). Also sample L-91 (no U–Pb data) yielded a similar Cpx–Pl age of 498 ± 7 ($^{87}Sr/^{86}Sr_{init} = 0.703356 \pm 0.000032$; $\varepsilon_{Sr} = -8.1$). Importantly, these isochron ages broadly correspond with the age of the host kimberlites (~500–600 Ma; Peltonen et al., 1999). This would suggest attainment of Sr-isotopic equilibrium between Pl and Cpx at the time of the kimberlite eruption and imply that the mafic granulites were at high ambient lower crustal temperatures at the time of the kimberlite magmatism. Stable conditions have prevailed within the craton margin since kimberlite magmatism (Kukkonen and Peltonen, 1999), and therefore the granulite xenoliths provide a close approximation of the present composition and physical state of the lower crust as well. The initial isotopic ratios cited above and ε_{Sr} (500) of −26.3 calculated from the Rb to Sr analysis on L-88 Cpx imply that the xenoliths have resided in an environment, which is characterized by low Rb/Sr ratios, i.e. typical lower crust.

Pb isotope analyses on Pl and Cpx are available on three samples (Table 3). In the $^{207}Pb/^{204}Pb$ versus $^{206}Pb/^{204}Pb$ diagram (not shown) they all plot below the Stacey and Kramers (1975) average terrestrial growth curve. The two Cpx–Pl pairs give imprecise age estimates of 1.9 ± 0.5 Ga (L87) and 0.8 ± 0.2 Ga (L91). The Pb isotope composition of plagioclase may be used to constrain the initial isotopic ratio of the rock. However, the timing of Pb closure remains unclear. It is likely, that the analytical data represent the Pb isotopic composition

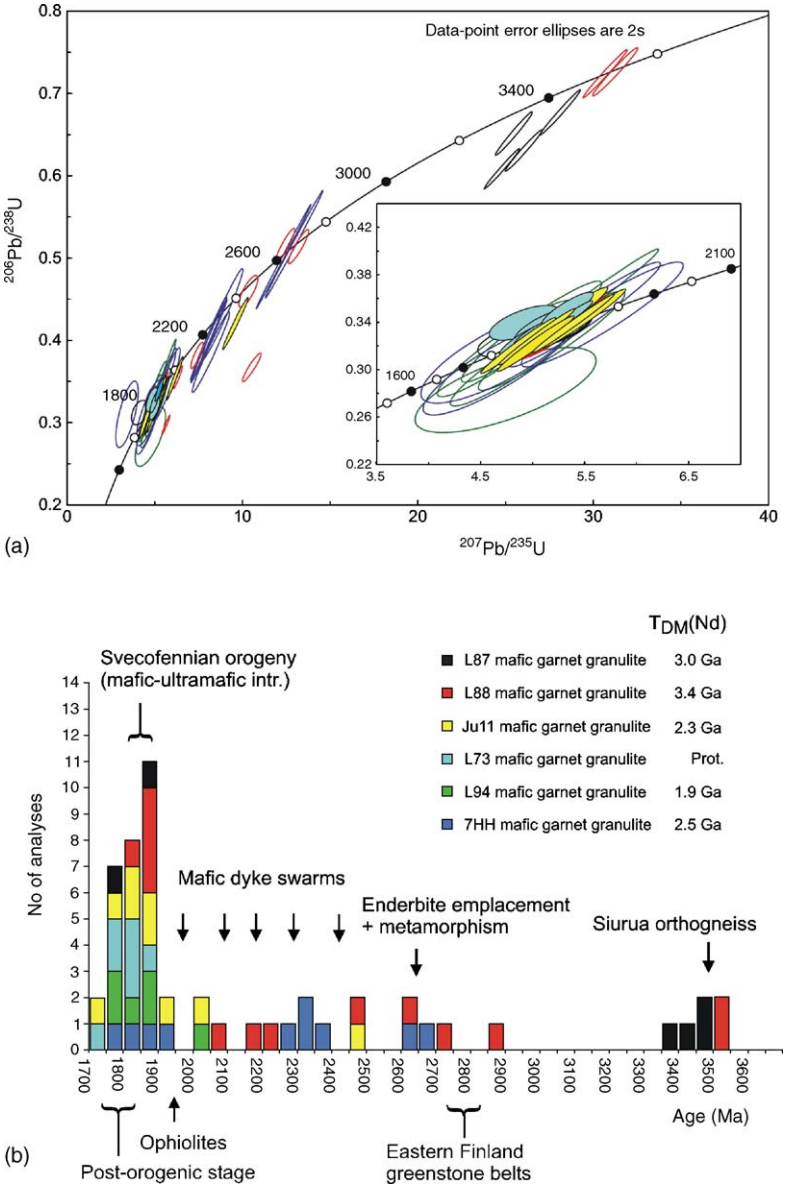

Fig. 4. (a) Concordia diagram and (b) histogram for $^{207}Pb/^{206}Pb$ ages showing NORDSIM U–Pb zircon data from 6 mafic granulite xenolith samples. Note that the data from each xenolith is indicated by the same colour in both diagrams. Important tectonic and magmatic events of the western part of the Karelian craton are indicated by vertical arrows.

of the rocks at ca. 1.6–1.9 Ga. The data especially from 7-HH Pl suggest that the rocks have evolved in a low U/Pb environment.

6. Discussion

6.1. Depth of origin and thermal history of the lower crustal xenoliths

One key issue in the study of granulite xenoliths is to ascertain whether the thermobarometric values they yield represent those that prevailed in the lower crust at the time of the host magmatism. Thermobarometric data reported by Hölttä et al. (2000) yielded the following equilibration conditions for the mineral assemblage Grt–Cpx–Pl–Qtz using mineral core compositions: $T = 802–925\,^{\circ}C$, $P = 0.84–1.25$ GPa. Geothermal constraints, however, imply that the lower crustal temperatures were significantly lower at the time of the kimberlite eruption. According to the geotherm determined by Kukkonen and Peltonen (1999), at 500–600 Ma the lower crustal temperatures ranged within 300–550 °C at

Table 3
Sm–Nd, Rb–Sr and Pb isotope results for mafic lower crustal xenoliths, Finland

Sample/ mineral	Sm (ppm)	Nd (ppm)	$^{147}Sm/^{144}Nd$ (±0.4%)	$^{143}Nd/^{144}Nd$	$2\sigma_m$	ε(1900)	T_{DM} (Ma)	T (Grt–Cpx) (Ma)	Rb (ppm)	Sr (ppm)	$^{87}Rb/^{86}Sr$	$^{87}Sr/^{86}Sr$	$2\sigma_m$	ε (500)	T (Cpx–Pl) (Ma)	$^{206}Pb/^{204}Pb$ (±0.15%)	$^{207}Pb/^{204}Pb$ (±0.15%)	$^{208}Pb/^{204}Pb$ (±0.15%)
L91 wr	2.93	9.95	0.1781	0.512313	10	−1.9	3240[a]											
L91 Grt	1.31	0.66	1.1970	0.523826	30	−25.9		1719 ± 9	0.49	0.33								
L91 Cpx	2.43	8.41	0.1743	0.512263	13	−1.9	3100[a]		3.10	16.64	0.5365	0.707163	20	−8.2		21.970	15.529	36.184
L91 Pl	0.12	0.97	0.0733						38.56	696.0	0.1597	0.704489	20	−8.1	498 ± 7	17.246	15.218	35.551
L87 Grt	3.75	1.97	1.1550	0.523002	40	−31.8		1692 ± 10	0.24	0.11								
L87 Cpx	6.86	27.29	0.1519	0.511841	10	−4.7	3000		2.39	27.09	0.2543	0.704450	40	−18.2				
L87 Pl	0.25	2.96	0.0511	0.510829	18	0.2			25.05	1051	0.0687	0.703250	30	−16.4	454 ± 20	16.210	15.192	35.512
L88 Cpx	6.88	27.07	0.1535	0.511742	10	−7.0	3370		2.55	91.09	0.0806	0.702640	40	−26.3		15.212	15.076	34.585
L73 Cpx	2.29	7.61	0.1817	0.512551	10	1.9	2350[a]											
JU11 wr	7.83	33.04	0.1433	0.511983	10	0.2	2290											
X001 wr	5.70	24.09	0.1430	0.511830	10	−2.7	2630											
X002 wr	12.01	50.88	0.1427	0.511994	13	0.5	2250											
L94 (2) wr	3.58	11.79	0.1834	0.512674	10	3.9	1844[a]											
L104 wr	4.41	17.07	0.1563	0.511690	20	−8.7	3700											
X208 wr	3.18	18.46	0.1041	0.511504	10	0.4	2130											
X029 wr	10.99	44.81	0.1483	0.511974	10	−1.2	2500											
L89 wr	5.81	23.40	0.1502	0.512133	30	1.4	2180											
7HH Pl#2	0.13	1.21	0.0671	0.511013	104	−0.1			49.9	626.9	0.2295	0.704741	20	−11.5		15.467	14.974	34.416
7HH wr[b]	5.02	21.60	0.1403	0.511852	10	−1.6	2480											
7HH Pl[b]	0.44	4.29	0.0626	0.511121	10	3.1												
7HH Cpx[b]	6.56	26.35	0.1505	0.511856	10	−4.1	2890											
7HH Grt[b]	2.12	1.25	1.0247	0.521072	22	−37.7		1604 ± 8										
L94 wr[b]	3.77	13.29	0.1717	0.512512	11	3.6	1920[a]											

T_{DM} according to DePaolo (1981), $2\sigma_m$ in the last significant digits.
7-HH Pl#2 was crushed and leached in hot 6 N HCl and HNO3.
[a] Large uncertainty due to high Sm/Nd.
[b] From Hölttä et al. (2000).

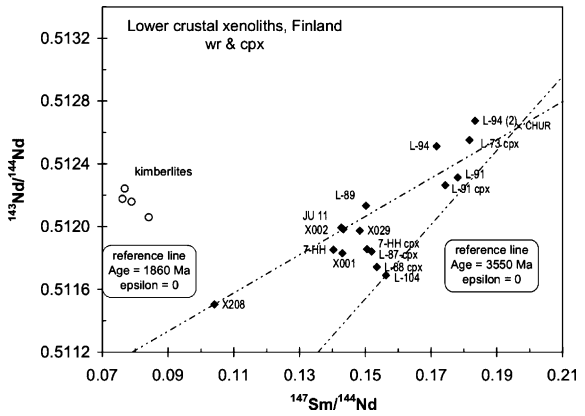

Fig. 5. $^{143}Nd/^{144}Nd$ vs. $^{147}Sm/^{144}Nd$ diagram for whole rock (wr) and clinopyroxene mineral separates (Cpx) of the lower crustal granulite xenoliths from Kaavi-Kuopio kimberlites in eastern Finland. Sm–Nd data of kimberlites from Peltonen et al. (1999).

30 and 60 km depths, respectively. The present lower crust is only slightly cooler due to decay of the heat-producing elements since 500–600 Ma. The ~+350 °C offset of the xenoliths from the geotherm clearly indicates that the calculated *P–T* values do not correspond to the lower crustal conditions at 500–600 Ma. A notable feature of these *PT*-data is that most of the values cluster close to 1.0 GPa and 825 °C, only couple of samples recording higher pressures up to 1.2 GPa (Hölttä et al., 2000). For the applied reaction grossular + pyrope + quartz = anorthite + diopside the dP/dT slope increases at higher pressures so that isobaric cooling of the sample from 925 to 800 °C would result in a

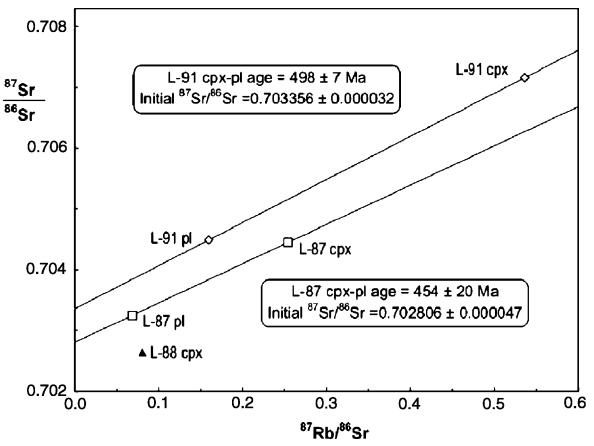

Fig. 6. $^{87}Sr/^{86}Sr$ vs. $^{87}Rb/^{86}Sr$ diagram for clinopyroxene and plagioclase mineral separates from lower crustal xenoliths L91 and L87. Note that mineral isochron ages are close to 500 Ma and broadly correspond to that of the kimberlite emplacement implying isotopic homogenisation of minerals and derivation of xenoliths from high ambient temperatures that characterise the lowermost crust.

~0.15 GPa decrease in the calculated pressure (Essene, 1989). This suggests that the clustering of the *P–T* values may well represent the closure of the Fe–Mg–Ca diffusion at ca. 800 °C, and that most of the samples are in fact derived from deeper levels than indicated by the calculated pressures. Accordingly, also the maximum value of 1.25 GPa probably underestimates the true maximum pressure, because the garnets are compositionally zoned and their cores do not show a clear compositional plateau and may also have been re-equilibrated.

Perhaps the most definitive evidence for derivation of a xenolith from the lower crust is the isotopic homogenisation of minerals, yielding ages equal to eruptive ages (Rudnick, 1992). Two-point clinopyroxene–plagioclase Rb–Sr ages determined for two samples are close (450 and 500 Ma) to that of the kimberlite emplacement (500–600 Ma), indicating that garnet granulites were derived at crustal depths, where ambient temperatures exceed the Rb–Sr blocking temperatures of these minerals – especially Cpx – at the time of kimberlite magmatism (Fig. 6). Blocking temperature for Sr diffusion in clinopyroxene is probably at least as high as that of phengite (≥500 °C; e.g. El-Shazly et al., 2001), which according to the xenolith-controlled present geotherm (Kukkonen and Peltonen, 1999) would locate the garnet granulites at ≥50 km depth in the present crust. Such depths indicate their derivation from relatively close to the seismic Moho and within the seismically determined high-velocity layer (Fig. 1b).

Further constraints on the thermal history of the garnet granulites is provided by mineral isochron ages. Sm–Nd Grt–Cpx isochron ages are considerably younger (~1600–1700 Ma) than the Proterozoic thermal overprinting on the craton, and thus must record some later process (Table 3). Since there is a considerable range in the isochron ages, and no evidence for major igneous events at that time, we interpret these ages to record the time interval when garnet granulites (at variable depths) passed the ~600–650 °C blocking temperature of garnet (Mezger et al., 1992; Ganguly et al., 1998).

In summary, these pressure estimates, together with the mineralogical compositions, P-wave velocities, and V_P/V_S ratios calculated for the xenoliths that match with those estimated from seismic wide-angle velocity models for the lower crust (Kuusisto et al., 2006), implies that the sample suite is derived from a deep, dense, mafic high-velocity layer (to compare V_P values see Table 1 and Fig. 1). Exact locations of extraction within the high-velocity layer cannot be constrained but probably granulites represent a range of depths. The fact that

our sample suite contains both Archean and Proterozoic granulites, is probably indicative that many samples are derived from the upper part of the high-velocity layer, and sample the transition zone between pre-existing Archean mafic garnet granulites and Proterozoic basaltic underplate. The age of the (latest) high temperature event recorded by the xenoliths is believed be Proterozoic, being directly dated by the clear, unzoned, low-U "metamorphic" zircon grains (Fig. 3a and d). Whether some of the older zircons actually date the Archean granulite-facies metamorphism remains uncertain, but we note the small peak at ~2600 Ma (Fig. 4b)—an event of regional metamorphism in the exposed cratonic terrain (Mänttäri and Hölttä, 2002). Overall, the petrological, thermal and geochronological evidence is most consistent with the mafic granulites representing Archean and Proterozoic mafic magmas, which once ponded and crystallised at lower crustal levels, have since remained within the deep crust. This view is further supported by the distinctly unradiogenic Sr and Pb isotopic compositions, which imply that the granulites have resided for a considerable time in a low-Rb/Sr, low-U/Pb environment, i.e. typical lower crust. One implication of the presence of very old mafic garnet granulites in our sample set is, that the generation of continental crust during the Paleoarchean did indeed leave behind a mafic lower crust. Most Archean cratons, however, do not have extensive Archean mafic lower crust (Rudnick and Gao, 2005), probably because it has been reworked by post-Archean basaltic underplating. This process seem to have been incomplete at the Karelian craton margin.

6.2. *Birth of the Karelian tectosphere and worldwide significance of the 3.5 Ga event*

Ancient, up to 3.55 Ga zircon ages, supported by the up to 3.7 Ga T_{DM} ages, imply that some of the studied granulite xenoliths from the Karelian cratonic lower crust represent the primary crust of the European continent. Equally old ages have only been reported from the Ukrainian shield, where 3.5–3.6 Ga zircons were analysed from tonalites and pyroxenites of the Novopavlovsk complex (Bibikova and Williams, 1990), and from Siurua (Finland) some 200 km NNW from the locality of the host kimberlites (Mutanen and Huhma, 2003; Fig. 1a). The data from Siurua are particularly relevant, because it implies that ≥3.5 Ga old igneous rocks, trondhjemitic orthogneiss and mafic garnet granulite, occur at present upper and lower crustal levels, respectively.

Major crustal growth episodes have been shown to accompany concomitant stabilisation of the underlying lithospheric mantle (Pearson, 1999). The chemical composition of the Karelian mantle has been reasonably well characterised based on mantle xenoliths and xenocrysts from the same kimberlites from where our lower crustal granulite xenoliths were recovered (Peltonen et al., 1999; Lehtonen et al., 2004). These studies imply that the 250-km-thick lithospheric mantle is compositionally stratified consisting of three texturally and compositionally distinct layers. While the "shallow layer" (from Moho to 110 km deep) and the "deep layer" (180–240 km) bear evidence of Proterozoic reworking due to proximity to the craton margin, the "middle" mantle layer (from 110 to 180 km depth) has yielded osmium isotopic ratios indicative of stabilisation at ~3.3 Ga (Peltonen and Brügmann, 2006). This age broadly corresponds not only to the oldest ages from our granulite xenoliths, but also with the age of the oldest upper crustal orthogneisses (Mutanen and Huhma, 2003), and the possibility exists that all these samples represent remnants of the Paleoarchean tectosphere that has remained coupled since its origin. Most of the early crust has, however, been reworked by later Archean processes. The fact that lower crustal samples yield also post-Archean protolith ages, does not require crust–mantle decoupling. This is because basic magmas from distant magmatic centers may be laterally migrated over hundreds of kilometers along the crust–mantle interface (Davis, 1997).

For a long time it has been recognised that crustal growth has been episodic in nature through Earth's history (e.g. Gastil, 1960), the most important events being 2.7, 1.9, and 1.2 Ga (Condie, 2001). Data from the Paleoarchean is fragmentary, but evidence which emphasises the importance of the ~3.5 Ga event is emerging. The cratons which show undeniable evidence for ~3.5 Ga growth of felsic continental crust include Kaapvaal (Armstrong et al., 1990), Pilbara (Buick et al., 1995), Wyoming (Mueller et al., 1996), Ukraine (Bibikova and Williams, 1990), Superior (Böhm et al., 2000), North China (Zheng et al., 2004), and now also Karelia in Fennoscandia (this study; Mutanen and Huhma, 2003). This is also the age of the oldest cratonic-type mafic dyke swarms, indicative of the existence of stable continental nuclei (Nutman et al., 1996). Notably, Re–Os isotope ratios of mantle sulphides included in silicates and diamonds from Kaapvaal and Siberian cratonic mantle xenoliths yielded Re–Os model ages (T_{MA}) that statistically cluster at 3.5 Ga (Pearson et al., 1999; Griffin et al., 2003), implying the existence of more than ~150 km thick cratonic roots at ~3.5 Ga—and by corollary the presence of abundant (and thick?) continental crust at that time. We suggest that the 3.5 Ga event represents a major mantle-plume event, when a significant fraction of juvenile Paleoarchean continental crust was created.

6.3. Reworking and hybridisation of the lower crust

A noteworthy feature is that mafic granulite xenoliths with Archean Sm–Nd (T_{DM}) protolith ages (L87, L88, and 7HH) yielded also a range of Proterozoic zircon ages that frequently lie along the concordia (Fig. 4a). Most of the post-Archean grains give dates that correspond to the Svecofennian orogeny at 1.85–1.90 Ga. Several grains also record intermediate ages between the Paleoarchean and Svecofennian "endmembers" (Fig. 4). There is general tendency that younger zircons show progressively fewer planar crystal faces and the less obvious zoning. This is most consistent with incomplete resetting of igneous zircon with some "memory" of the protolith composition remaining (Hoskin and Black, 2000). Since intermediate ages seem to coincide with major events of basic magmatism within the craton (e.g. Vuollo and Huhma, 2005), we interpret that solid-state recrystallisation of older – variably metamictised – grains took place due to episodic, instead of continuous (Ashwal et al., 1999) lead loss. In contrast, all zircons that give younger (Svecofennian) ages seem to record more advanced stages of recrystallisation: they are colorless, isometric to oval, unzoned, and have very low-U contents (6–16 ppm). These are characteristic features of zircons re-equilibrated at granulite facies temperatures (e.g. Vavra et al., 1999). The preservation of number of geologically meaningful Proterozoic ages in small Archean xenolith samples [(Nd(T_{DM}) > 3 Ga] is a result of a combination of the response of zircons to transient heating in the low-U, lower crustal environment and their subsequent storage at the high ambient temperature. Recrystallised grains tend to incorporate only little uranium and therefore become resistant to further recrystallisation (Pidgeon, 1992). The younger the zircon generation is, the more likely it will remain intact in subsequent thermal pulses. A corollary is that the oldest grains preferentially tend to recrystallise in each event, which explains their low proportion in the Archean protoliths. Ambient lower crustal temperatures in the Karelian lower crust have been high enough to constantly heal the metamictic damage of the zircon, resulting in concordant data (Pidgeon, 1992). The presence of zircons yielding a large range of ages within small xenoliths is an intriquing problem (e.g. $^{207}Pb/^{206}Pb$ ages of L88 range from 3532 to1842 Ma), even more so, if Proterozoic overgrowths are not present on older grains. One explanation would be that the preservation of zircon grains depends on the mineral in which they are enclosed. For example, zircons completely encapsulated by quartz or plagioclase are protected by their Zr- and volatile-free host phase, while zircons enclosed by e.g. amphibole are more prone to solid-state recrystallisation during metamorphism.

A clear positive correlation exists between the Sm and Nd model age (T_{DM}) and the age of the oldest zircons found in a sample (Fig. 4). This is considered as strong evidence that the oldest zircon ages date the protolith crystallisation, and also that when younger zircons are present in the same sample they represent recrystallised older grains. Several of the samples record only Proterozoic Nd model (2.3–1.9 Ga) and zircon ages (2.5–1.7 Ga), implying that the present lower crust consists of both Archean and Proterozoic granulites. We consider it hybrid in nature, where Archean mafic lower crust has been repeatedly intruded by Proterozoic mafic magmas in multiple events. These events seem to have their expressions also at presently exposed crustal levels in the form of layered intrusions, dike swarms and lava fields (Fig. 4b). However, one major event of basic magmatism, i.e. the ~2.8 Ga formation of the eastern Finland greenstone belts with abundant tholeiitic and komatiititc volcanism, is not recorded by lower crustal zircons. Complete lack of such dates in our lower crustal granulite samples probably indicates that these greenstone belts do not represent rift-related formations (Luukkonen, 1992), but rather allochthonous nappes (klippes) derived from oceanic plateaus—an origin proposed also for the Kostomuksha greenstone belt some 80 km east of Kuhmo-Suomussalmi (Puchtel et al., 1998).

The age histogram (Fig. 4b) implies that the Svecofennian orogeny ~1.92–1.85 Ga was not the last episode that affected the lower crust. Nearly half of all analysed zircon grains give dates younger than the orogeny (<1.85 Ga) and occur in both Proterozoic and Archean protoliths. Importantly, these post-orogenic grains show only ghost-like internal structures and are oval-shape and low in U (Fig. 3b–d). The gradual decrease in the stability of planar crystal faces, together with their similarity on size with older grains, precludes their origin by breakdown of a zirconium-bearing phase such as amphibole (Fraser et al., 1997). Although the post-orogenic <1.85 Ga grains are abundant, we find no conclusive evidence for addition of new basaltic material to the lower crust at that time, because all samples with post-orogenic zircons also have grains that record ages at least as old as the Svecofennian orogeny. Therefore, we interpret *all* post-orogenic grains to represent older grains that recrystallised at an event when lower crust remained intact, but was transiently heated, probably by magmas ponded at somewhat deeper levels, perhaps within uppermost mantle. Direct evidence for such magmas include 1.8 Ga zircon xenocrysts – terpreted to originate from hydrous veins in the uppermost

mantle peridotite – in the host kimberlites (Peltonen and Mänttäri, 2001) and ~1.8 Ga post-orogenic granites and lamprophyres in the region (e.g. Patchett and Kouvo, 1986; Eklund et al., 1998). Finally, the 1724 Ma overgrowth on Ju11 zircons (Fig. 3c) is a clear indication of an even younger event which has no expressions in the exposed geology of the Karelian craton. Interestingly, similar U–Pb zircon ages were obtained by Downes et al. (2002) for lower crustal xenoliths from the Elovy Island diatreme, Kola Peninsula, corresponding with the ages of upper crustal granites in that region. Probably, this was an extensive event that extended also to the Karelian craton margin, its thermal effects being, however, restricted to lower crustal levels.

7. Conclusions

Granulite xenoliths recovered from Kaavi-Kuopio kimberlites provide a unique access to the chemical composition and physical properties of the craton margin lower crust. Thermobarometry, isotopic homogenisation of minerals, and seismic velocity constraints all imply that our sample suite indeed represents the lower crust at the time of the kimberlite emplacement at ~500–600 Ma. Within this stable shield area these samples also provide a close approximation of the present lower crust. The lowermost crust mainly consists of mafic garnet granulites with minor amounts of orthopyroxene-bearing gabbros and felsic granulites. This xenolith suite includes Archean mafic granulites that yielded zircon ages of up to ~3.5 Ga and Nd T_{DM} model ages up to ~3.7 Ga. These samples are among the oldest reported from lower crust anywhere, and are interpreted as remnants of the mafic lower crust of the Paleoarchean protocraton. Much of this ancient lower crust was obliterated by Paleoproterozoic basaltic underplating that most of the samples represent. Extensive emplacement of basaltic magmas at the crust–mantle interface occurred during the Svecofennian orogeny at ~1.9 Ga, but several xenoliths also record evidence of transient post-orogenic heating episodes, that do not all have their expressions at exposed crustal levels.

Acknowledgements

Laboratory staff at Nordsim (Stockholm) and Geological Survey of Finland (Espoo), Lev Ilyinsky, Kerstin Lindén and Tuula Hokkanen are thanked for their skilled analytical assistance. The Nordsim facility is operated and funded under an agreement between the research councils of Sweden, Denmark and Norway, and the Geological Survey of Finland and Swedish Museum of Natural History. M.M. Raith and an anonymous journal referee are thanked for their thorough and helpful reviews. This is Nordsim contribution #144.

References

Armstrong, R.A., Compston, W., de Wit, M.J., Williams, I.S., 1990. The stratigraphy of the 3.5–3.2 Ga Barberton greenstone belt revisited; a single zircon ion microprobe study. Earth Planet. Sci. Lett. 101, 90–106.

Ashwal, L.D., Tucker, R.D., Zinner, K., 1999. Slow cooling of deep crustal granulites and the Pb-loss in zircon. Geochim. Cosmochim. Acta 63, 2839–2851.

Bibikova, E.V., Williams, I.S., 1990. Ion microprobe U–Th–Pb isotopic studies of zircons from three early Precambrian areas in the USSR. Precambrian Res. 48, 203–221.

Böhm, C.O., Heaman, L.M., Creaser, R.A., Corkery, M.T., 2000. Discovery of pre-3.5 Ga exotic crust at the northwestern Superior Province Manitoba. Geology 28, 75–78.

Buick, R., Thornett, J.R., McNaughton, N.J., Smith, J.B., Barley, M.E., Savage, M., 1995. Record of emergent continental crust ~3.5 Ga billion years age in the Pilbara craton of Australia. Nature 375, 574–577.

Claesson, S., Huhma, H., Kinny, P.D., Williams, I.S., 1993. Svecofennian detrital zircon ages—implications for the Precambrian evolution of the Baltic Shield. Precambrian Res. 64, 109–130.

Condie, K.C., 2001. Mantle Plumes and their Record in Earth History. Cambridge University Press, p. 366.

El-Shazly, A.K., Broecker, M., Hacker, B., Calvert, A., 2001. Formation and exhumation of blueschists and eclogites from NE Oman; new perspectives from Rb–Sr and 40 Ar/39 Ar dating. J. Metamorph. Geol. 19, 233–248.

Eklund, O., Konopelko, D., Rutanen, H., Frödjö, S., Shebanov, A.D., 1998. 1.8 Ga Svecofennian post-collisional shoshonitic magmatism in the Fennoscandian shield. Lithos 45, 87–108.

Essene, E.J., 1989. The current status of thermobarometry in metamorphic rocks. In: Daly, et al. (Eds.), Evolution of Metamorphic Belts, vol. 43. Geol. Soc. Spec. Publ, pp. 1–44.

DePaolo, D.J., 1981. Neodymium isotopes in the Colorado Front Range and crust–mantle evolution in the Proterozoic. Nature 291, 193–196.

Davis, W.L., 1997. U–Pb zircon and rutile ages from granulite xenoliths in the Slave province: Evidence for mafic magmatism in the lower crust coincident with Proterozoic dike swarms. Geology 25, 343–346.

Downes, H., Peltonen, P., Mänttäri, I., Sharkov, E.V., 2002. Proterozoic zircon ages from lower crustal granulite xenoliths, Kola Peninsula Russia: Evidence for crustal growth and reworking. J. Geol. Soc. Lond. 159, 485–488.

Fraser, G., Ellis, D., Eggins, S., 1997. Zirconium abundance in granulite-facies minerals, with implications for zircon chronology in high-grade rocks. Geology 25, 607–610.

Ganguly, J., Tirone, M., Hervig, R.L., 1998. Diffusion kinetics of samarium and neodymium in garnet, and a method for determining cooling rates of rocks. Science 281, 805–807.

Gastil, G., 1960. The distribution of mineral dates in space and time. Am. J. Sci. 258, 1–35.

Griffin, W.L., O'Reilly, S.Y.O., Abe, N., Aulbach, S., Davies, R.M., Pearson, N.J., Doyle, B.J., Kivi, K., 2003. The origin and evolution of Archean lithospheric mantle. Precambrian Res. 127, 19–41.

Hoskin, P.W.O., Black, L.P., 2000. Metamorphic zircon formation by solid-state recrystallization of protolith igneous zircon. J. Metamorph. Geol. 18, 423–439.

Hölttä, P., Huhma, H., Mänttäri, I., Peltonen, P., Juhanoja, J., 2000. Petrology and geochemistry of mafic granulite xenoliths from the Lahtojoki kimberlite pipe, eastern Finland. Lithos 51, 109–133.

Kempton, P.D., Downes, H., Neymark, L.A., Wartho, J.A., Zartman, R.E., Sharkov, E.V., 2001. Garnet granulite xenoliths from the northern Baltic Shield—the underplated crust of a Palaeoproterozoic large igneous province? J. Petrol. 42, 731–763.

Korsman, K., Korja, T., Pajunen, M., Virransalo, P., GGT/SVEKA Working Group, 1999. The GGT/SVEKA transect: structure and evolution of the continental crust in the Palaeoproterozoic Svecofennian orogen in Finland. Int. Geol. Rev. 41, 287–333.

Kukkonen, I.T., Peltonen, P., 1999. Xenolith-controlled geotherm for the central Fennoscandian Shield: implications for lithosphere–astenosphere relations. Tectonophysics 304, 301–315.

Kuusisto, M., Kukkonen, I., Heikkinen, P., Pesonen, L.J., 2006. Lithological interpretation of crustal composition in the Fennoscandian Shield with seismic velocity data. Tectonophysics.

Lehtonen, M., O'Brien, H.E., Peltonen, P., Johanson, B.S., Pakkanen, L.K., 2004. Layered mantle at the Karelian craton margin: *P–T* of mantle xenocrysts and xenoliths from the Kaavi-Kuopio kimberlites Finland. Lithos 77, 593–608.

Ludwig, K.R., 2001. Isoplot/Ex rev. 2.49. A geochronological toolkit for Microsoft Excel. Berkeley Geochronology Center. Special Publication No. 1a.

Luukkonen, E.J., 1992. Late Archaean and early Proterozoic structural evolution in the Kuhmo-Suomussalmi terrain, eastern Finland. University of Turku, Series A. II. Biolog. Geogr. Geol. 78, 115.

Mänttäri, I., Hölttä, P., 2002. U–Pb dating of zircons and monazites from Archean granulites in Varpaisjärvi, central Finland: evidence for multiple metamorphism and Neoarchean terrane accretion. Precambrian Res. 118, 101–131.

Markwick, A.J.W., Downes, H., 2000. Lower crustal granulite xenoliths from the Arkhangelsk kimberlite pipes: petrological, geophysical and geochemical constraints. Lithos 51, 135–151.

Mezger, K., Essene, E.J., Halliday, A.N., 1992. Closure temperature of the Sm–Nd system in metamorphic garnets. Earth Planet. Sci. Lett. 113, 397–409.

Mezger, K., Krogstad, E.J., 1997. Interpretation of discordant U–Pb zircon ages: an evaluation. J. Metamorph. Geol. 15, 127–140.

Mueller, P.A., Wooden, J.L., Mogk, D.W., Nutman, A.P., Williams, I.S., 1996. Extended history of a 3.5 Ga trondhjemitic gneiss, Wyoming province USA: evidence from U–Pb systematics in zircon. Precambrian Res. 78, 41–52.

Mutanen, T., Huhma, H., 2003. The 3.5 Ga Siurua trondhjemite gneiss in the Archean Pudasjärvi Granulite Belt, northern Finland. Bull. Geol. Soc. Finland 75, 51–68.

Nironen, M., 1997. The Svecofennian orogen. Precambrian Res. 86, 21–44.

Nutman, A.P., McGregor, V.R., Friend, C.R.L., Bennett, V.C., Kinny, P.D., 1996. The Itsaq gneiss complex of southern West Greenland: the worlds most extensive record of early crustal evolution (3900–3600 Ma). Precambrian Res. 78, 1–39.

O'Brien, H.E., Tyni, M., 1999. Mineralogy and geochemistry of kimberlites and related rocks from Finland. In: Gurney, J.J., et al. (Eds.), Proceedings of the Seventh International Kimberlite Conference, vol. 2. University of Cape Town, Cape Town, South Africa, pp. 625–636.

Pearson, D.G., 1999. The age of continental roots. Lithos 48, 171–194.

Pearson, D.G., Shirey, S.B., Bulanova, G.P., Carlson, R.W., Milledge, H.J., 1999. Single crystal Re–Os isotope study of sulphide inclusions from a zoned Siberian diamond. Geochim. Cosmochim. Acta 63, 703–712.

Patchett, J., Kouvo, O., 1986. Origin of continental crust of 1.9–1. 7 Ga age: Nd isotopes and U–Pb zircon ages in the Svecokarelian terrain of South Finland. Contrib. Miner. Petrol. 92, 1–12.

Peltonen, P., Huhma, H., Tyni, M., Shimizu, N., 1999. Garnet peridotite xenoliths from kimberlites of Finland: nature of the continental mantle at an Archaean craton–Proterozoic mobile belt transition. In: Gurney, J.J., et al. (Eds.), Proceedings of the Seventh International Kimberlite Conference, vol. 2. University of Cape Town, Cape Town, pp. 664–676.

Peltonen, P., Mänttäri, I., 2001. An ion microprobe U–Th–Pb study of zircon xenocrysts from the Lahtojoki kimberlite pipe, eastern Finland. Bull. Geol. Soc. Finland 73, 47–58.

Peltonen, P., Kontinen, A., 2004. The Jormua ophiolite: a mafic–ultramafic complex from an ancient ocean–continent transition zone. In: Kusky, T.M. (Ed.), Precambrian Ophiolites and Related Rocks. Developments in Precambrian Geology, vol. 13. Elsevier B.V., pp. 35–71 (Condie, K.C., Series Editor).

Peltonen, P., Brügmann, G., 2006. Origin of layered continental mantle (Karelian craton, Finland): geochemical and Re–Os isotope constraints. Lithos.

Pidgeon, R.T., 1992. Recrystallisation of oscillatory zoned zircon: Some geochronological and petrological implications. Contrib. Miner. Petrol. 110, 463–472.

Puchtel, I.S., Hofmann, A.W., Mezger, K., Jochum, K.P., Shchipansky, A.A., Samsonov, A.V., 1998. Oceanic plateau model for continental crustal growth in the Archean: a case study from the Kostomuksha greenstone belt NW Baltic Shield. Earth Planet. Sci. Lett. 155, 57–74.

Puchtel, I.S., Hofmann, A.W., Amelin, Yu.V., Garbe-Schönberg, C.-D., Samsonov, A.V., Shchipansky, A.A., 1999. Combined mantle plume-island arc model for the formation of the 2.9 Ga Sumozero-Kenozero greenstone belt SE Baltic Shield: Isotope and trace element constraints. Geochim. Cosmochim. Acta 63, 3579–3595.

Rudnick, R.L., 1992. Xenoliths—samples of lower continental crust. In: Fountain, D.M., et al. (Eds.), The Continental Lower Crust. Developments in Geotectonics, vol. 23. Elsevier, Amsterdam, pp. 269–316.

Rudnick, R.L., Gao, S., 2005. Composition of the continental crust. In: Rudnick, R.L. (Ed.), The Crust. Treatise on Geochemistry, vol. 3. Elsevier–Pergamon, Oxford, pp. 1–64.

Shchipansky, A.A., Samsonov, A.V., Bibikova, E.V., Babarina, I.I., Konilov, A.N., Krylov, K.A., Slabunov, A.I., Bogina, M.M., 2004. 2.8 Ga boninite-hosting partial suprasubduction zone ophiolite sequences from the North Karelian greenstone belt, NE Baltic Shield, Russia. In: Kusky, T.M. (Ed.), Precambrian Ophiolites and Related Rocks. Developments in Precambrian Geology, vol. 13. Elsevier B.V., pp. 425–486 (Condie, K.C., Series Editor).

Sorjonen-Ward, P., Luukkonen, E., 2005. Archean rocks. In: Lehtinen, M., et al. (Eds.), Precambrian Geology of Finland—Key to the Evolution of the Fennoscandian Shield. Elsevier, Amsterdam, pp. 35–115.

Stacey, J.S., Kramers, J.D., 1975. Approximation of the terrestrial lead isotope evolution by a two-stage model. Earth Planet. Sci. Lett. 26, 207–221.

Vavra, G., Schmid, R., Gebauer, D., 1999. Internal morphology, habit and U–Th–Pb microanalysis of amphibole-to-granulite facies zircons: geochronology of the Ivrea Zone (Southern Alps). Contrib. Miner. Petrol. 134, 380–404.

Vuollo, J., Huhma, H., 2005. Paleoproterozoic mafic dikes in NE Finland. In: Lehtinen, M., et al. (Eds.), Precambrian Geology of Finland—Key to the Evolution of the Fennoscandian Shield. Elsevier, Amsterdam, pp. 193–235.

Whitehouse, M.J., Kamber, B., Moorbath, S., 1999. Age significance of U–Th–Pb zircon data from early Archean rocks of west Greenland—a reassessment based on combined ion-microprobe and imaging studies. Chem. Geol. 160, 201–224.

Wiedenbeck, M., Allé, P., Corfu, F., Griffin, W.L., Meier, M., Oberli, F., von Quadt, A., Roddick, J.C., Spiegeln, W., 1995. Three natural zircon standards for U–Th–Pb, Lu–Hf, trace element and REE analysis. Geostandards Newslett. 19, 1–23.

Zheng, J., Griffin, W.L., O'Reilly, S.Y., Lu, F., Wang, C., Zhang, M., Wang, F., Li, H., 2004. 3.6 Ga lower crust in central China: new evidence on the assembly of the North China craton. Geology 32, 229–232.